

# Tools for Assessment and Planning of Aquaculture Sustainability



SHORT TITLE:	TAPAS
COORDINATOR:	Prof. Trevor Telfer University of STIRLING, UK
ORGANISATION:	
TOPIC:	H2020- SFS-11b-2015
PROJECT NUMBER:	678396

## DELIVERABLE: 6.5

### Algorithm sets for Sentinel-3 OLCI relevant to a range of aquaculture environments

#### Contributing Authors:

Stephanie Palmer, Laurent Barillé, Pierre Gernez (University of Nantes)  
Stefan Simis, Benjamin Loveday (Plymouth Marine Laboratory)  
Marnix Laanen, Lazaros Spaias (Water Insight)

#### History of changes:

Ver	Date	Changes	Author
1	01/11/2019	Initial draft template	ML
2	20/12/2019	Final version	ML, PG, SS, BL
3	10/2/2020	Revised version	ML, PG, SS

#### Internal review

Date	Name
11/2/2020	Trevor Telfer



**Refer to this document as:**

M.L. Laanen, P. Gernez, S.C.J. Palmer, L. Barillé, S.G.H. Simis, B. Loveday. 2019. Algorithm sets for Sentinel-3 OLCI relevant to a range of aquaculture environments. EU H2020 TAPAS Deliverable 6.5. Report. 27 pp.

## TABLE OF CONTENTS

TABLE OF CONTENTS.....	3
1. Introduction .....	4
2. Regional tuning of TSM and Chl algorithms in Bourgneuf Bay, France (University of Nantes) .....	5
2.1. Background .....	5
2.2. Algorithm calibration and validation .....	5
2.3. Conclusion from the regional approach .....	7
3. <i>Calimnos</i> coastal water quality and optical typology (PML) .....	8
3.1. Background .....	8
3.2. Algorithm overview .....	8
3.3. Specific algorithms for <i>Calimnos</i> for coastal water quality .....	10
3.3.1. General considerations .....	10
3.3.2. Pixel identification .....	10
3.3.3. Atmospheric correction .....	11
3.4. Specific algorithms for derived water quality products.....	12
3.4.1. Optical water type (OWT) membership – overview .....	12
3.4.2. Generating a coastal optical water typology .....	12
3.4.3. Algorithm selection, tuning, calibration and validation: .....	16
3.4.4. Limitations, recommendations for use and further evolution of the algorithm .....	19
3.5. Output product .....	20
4. The S3 processing chain for Bourgneuf Bay (Water Insight) .....	22
4.1. Background .....	22
4.2. S3 processing chain .....	22
5. Conclusions and recommendations.....	24
6. References .....	25

## 1. Introduction

Aquaculture is predominantly found on land, in inland waterbodies and in the inshore to coastal environment. Water quality and temperature observations from satellites fulfil an important role in monitoring the aquatic environment, including the suitability for specific aquaculture activities and their potential impacts on their immediate environment.

This report presents a number of state-of-the-art approaches to using the latest generation of ocean colour sensors for water quality monitoring in environments relevant to aquaculture. Due to proximity to land, these waters are classified as optically complex, implying that the interpretation of water colour in terms of optical-biogeochemical substance concentrations is subject to ambiguity (the same colour can be interpreted in different ways). In addition, proximity to land adds uncertainty in the separation of water and atmospheric optical conditions, as well as disturbance of the water-leaving radiance signal by optically shallow (bottom visibility) and highly variable water surface conditions (waves and surf). The methodologies presented here are designed, to an extent, to overcome and/or recognize such conditions.

The methodologies that were optimized during TAPAS are described in the following sections, including aggregate maps of optical conditions and results for specific farm-scale case studies.

## 2. Regional tuning of TSM and Chl algorithms in Bourgneuf Bay, France (University of Nantes)

### 2.1. Background

The results presented here were published in the open access journal *Frontiers in marine sciences*, in the frame of the research topic “Remote Sensing for Aquaculture”:

<https://www.frontiersin.org/research-topics/9293/remote-sensing-for-aquaculture>

Bourgneuf Bay is a 340 km<sup>2</sup> macrotidal embayment located on the French Atlantic coast. There are currently 283 mainly small oyster farms occupying leases over approximately 10% of the 100 km<sup>2</sup> intertidal zone, producing Pacific oysters (*Crassostrea gigas*). Expanding production to the offshore environment has been of interest to Bourgneuf Bay farmers for some time now, as there is no more room to expand in the intertidal zone. Aquaculture is not necessarily feasible everywhere, however, and appropriate site selection for new farms is key to their success and sustainability. Several socioeconomic and environmental constraints need to be considered as part of spatial multi-criteria evaluation and marine spatial planning endeavors (Falconer et al., 2019). The biological growth potential for a given species is a key factor for site selection and is expected to vary spatially as a result of changes in environmental factors such total suspended matter (TSM) and chlorophyll-a (Chl) concentration.

In Bourgneuf Bay, strong spatial gradients in these parameters turbidity of the water column have been observed, with highly turbid conditions (TSM typically up to more than 300 g m<sup>-3</sup>) in the intertidal zone related to tidal- and wind-driven resuspension of surface sediment at shallower water depths, and relatively clear conditions offshore (TSM generally < 60 g m<sup>-3</sup>). Chl concentration in Bourgneuf Bay has also been reported to span several orders of magnitude, and typically ranges from < 5 mg m<sup>-3</sup> offshore to > 10 mg m<sup>-3</sup> in the intertidal zone (Gernez et al., 2017).

This section presents the TSM and Chl regional algorithms specifically developed and validated for Bourgneuf Bay. The associated EO-derived maps were then coupled with oyster physiological modelling to provide insight into the spatiotemporal variability underlying the biological potential, and thereby inform site selection for offshore oyster aquaculture in Bourgneuf Bay (Palmer et al., accepted).

### 2.2. Algorithm calibration and validation

The TSM and Chl algorithms were developed using in situ datasets (Palmer et al., accepted). A total of 46 and 62 matchups were eventually available for the calibration and validation of the TSM and Chl algorithms, respectively. The algorithms were developed for the ESA MEdium Resolution Imaging spectrometer (MERIS). Although more recent satellite data are available (i.e. Sentinel3 from 2015), these do not coincide with the in situ data (2005 - 2006)

needed for algorithm validation. MERIS data from 2003-2011 were therefore used here. The Full Resolution MERIS data were processed by PML using the Calimnos processing chain, which is designed to dynamically resolve optical water quality parameters in a variety of optically complex inland waters (Simis et al., 2018). Version 1.21 of the processing chain was applied to the 1934 Level 1B FR images available for our site from the period 2003-2011, including Polymer atmospheric correction with a mineral absorption model, the removal of flagged invalid and suspect pixels, and the application of Chl and TSM retrieval algorithms to obtain L2 products. The MERIS Chl and TSM products available through Calimnos and tuned to lake optical properties according to the water types described by Spyarakos et al. (2018) were not found to adequately match the concentrations measured in situ at our site, but several had robust linear relationships with the in situ data. We therefore recalibrated these algorithms for Bourgneuf Bay to improve confidence in the results and applied the recalibrated algorithms to the full time series of interest (Figure 1). The overall best performing algorithms for the detection of in-water constituents including both offshore and intertidal matchups (highest coefficient of determination,  $R^2$ , for model fit) were OC2 (O'Reilly et al., 2000) for Chl retrieval, which is a fourth-order polynomial relationship between the ratio of the MERIS band centered at 490 nm to that centered at 560 nm and Chl, and the Binding et al. (2010) algorithm for TSM, which uses the MERIS band centered at 754 nm in semi-analytical inverse modelling. Recalibration and validation of Chl and TSM retrieval algorithms was carried out by splitting the in situ data set into two groups at random; one (70%) to determine the tuning coefficients (i.e., recalibration) and the other (30%) to assess how accurately the tuned algorithm retrieved the absolute concentrations (i.e., validation).

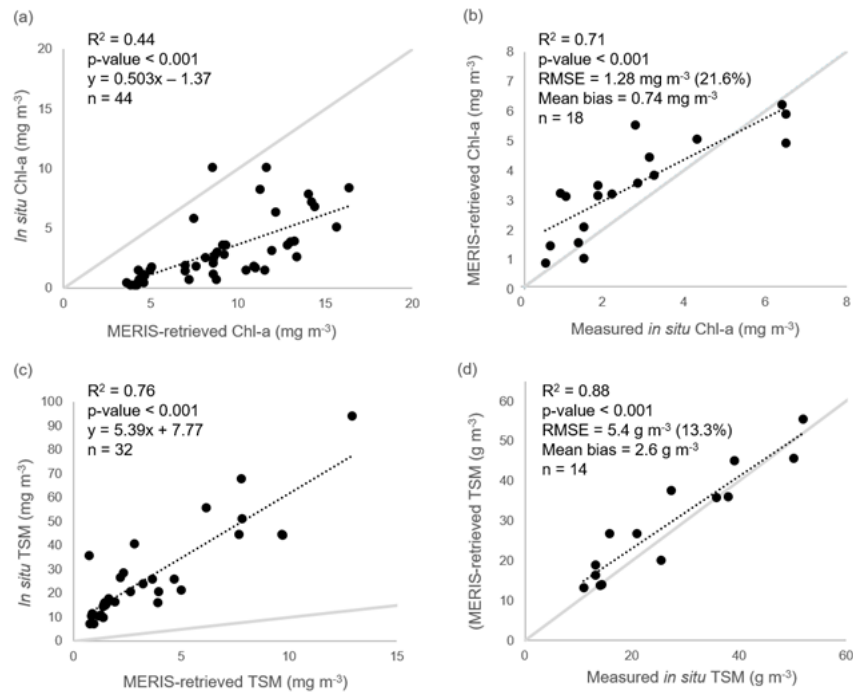


Figure 1: Recalibration (a, c) and validation (b, d) of MERIS OC2 Chl-a (a, b) and Binding et al. (2010) TSM (c, d) retrieval algorithms (from Palmer et al., accepted).

### 2.3. Conclusion from the regional approach

As the Ocean Land Colour Instrument (OLCI) onboard Sentinel 3 has been designed to provide a consistent continuity with MERIS, the algorithms developed here for MERIS would similarly apply to Sentinel 3. While simple regional tuning of EO observations can provide accurate TSM and Chl products for aquaculture applications, as demonstrated here in Bourgneuf Bay, the validity of such an approach depends on the existence of in situ data and is restricted to the conditions encountered in the in situ measurements. In the next section, a more generalized framework is presented for the provision of more globally valid products.

### 3. *Calimnos* coastal water quality and optical typology (PML)

#### 3.1. Background

The *Calimnos* processing chain was initially developed for the UK-based GloboLakes project, in turn based on the first global inland waterbodies processing chain using a comprehensive library of algorithms and resultant products in the ESA Diversity-2 project. These processing chains were built to process archived ENVISAT-MERIS data at full resolution (300m).

*Calimnos* is a versatile processing environment capable of handling Sentinel-3 OLCI, Sentinel-2 MSI, Aqua-MODIS and Envisat-MERIS satellite data. It can be run on data archives to produce time-series, or in operational mode in a high-performance computing environment. It is presently used to deliver the Copernicus Land Monitoring Service (CLMS) – Lake water quality products (LWLR, Turbidity, Trophic State Index) at 10-day aggregation intervals, and it is also the processing environment for the Lakes Essential Climate Variable Lake-water-leaving reflectance (LWLR) generated in the ESA Climate Change Initiative. In this configuration it uses a set of algorithms optimised to retrieve water-column properties in a wide range of lakes.

Within TAPAS an algorithm configuration was developed for water quality retrieval in coastal seas. Part of this work focused on using the high-resolution Sentinel-2 MSI sensor and aligning its retrieval with coincident observations from the ocean colour sensor OLCI onboard Sentinel-3, to ultimately arrive at seamless integration from inshore (requiring high resolution observation) to offshore environments (requiring higher radiometric sensitivity offered by ocean colour sensors). The remaining work, described in the current report, is concerned with optimising *Calimnos* for coastal areas. New elements are (1) the determination of coastal optical water types, to which (individually calibrated) constituent retrieval algorithms are mapped, and (2) optimized retrieval of Turbidity across these optical water types.

It should be noted that *Calimnos* is a processing chain with multiple processing stages and algorithms, described in documents referred to in the following sections. The algorithms that form the core of atmospheric correction and retrieval of water column optical properties are based on published literature whereas algorithm-specific tuning and their assignment to specific optical water types is unique to *Calimnos*.

#### 3.2. Algorithm overview

*Calimnos* combines data discovery, subsetting by target area (individual water bodies), radiometric and atmospheric corrections, pixel identification (land/cloud/water/ice), optical water type classification, individual algorithms (per parameter and water type), algorithm blending, conversion and aggregation into a single processing chain.

A schematic overview of *Calimnos* is given in Figure 1. The main processing stages and their corresponding algorithms are given below.



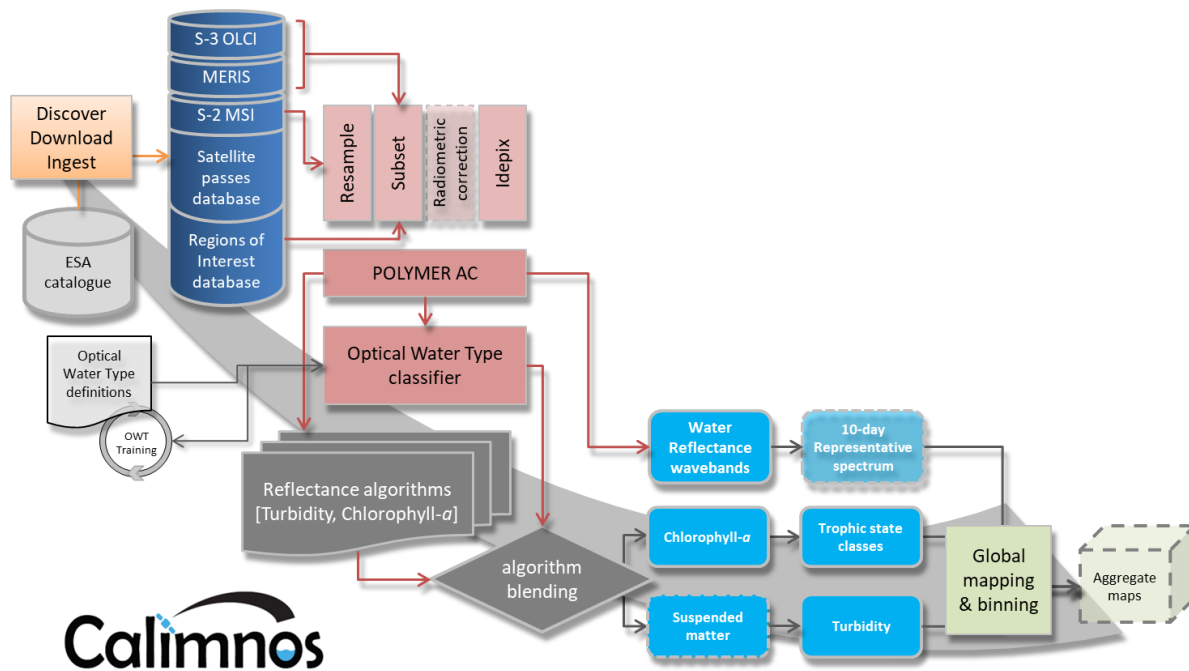


Figure 2: Schematic overview of the *Calimnos* processing chain.

To produce Lake Water-Leaving Reflectance:

- Data discovery. Following download of new satellite passes at L1B these are entered into a geospatial database. Target regions are similarly specified in a geospatial database and satellite products which overlap any of the target regions are queued for processing. In the context of re-processing, any duplicate passes are removed. The procedure relies on in-house python scripts and postgres database functionality.
- Subsetting. For best processing performance, satellite passes are subsetting to bounding boxes around each target area. The subsetting routine is part of the SNAP toolbox, called through the Graph Processing Tool (GPT).
- Radiometric corrections. Any radiometric ('gain') corrections defined following the release of the data are applied to the L1B imagery before submitting the data to atmospheric correction.
- Pixel identification. The *Idepix* neural network routine is applied for initial pixel identification as water, land, cloud/haze, or snow/ice. *Idepix* is called through SNAP using the GPT. Pixel identification masks are stored for later masking of invalid (non-water) pixels.
- Atmospheric correction. POLYMER is applied to the corrected L1B data of MERIS and OLCI sensors and yields water-leaving reflectance wavebands. The outputs are fully normalized water-leaving reflectance per waveband. POLYMER is called using a function wrapper in Python.

To produce derived water-column properties:

- Optical water type classification. An optical water type (OWT) classification for coastal waters was developed under projects TAPAS and Orsect (Loveday et al. in prep). Distance metrics between the atmospherically corrected observation and each water type are generated for each pixel.
- Algorithm mapping and blending. For each OWT a best-performing algorithm (see section 4) is mapped. The algorithms results are then blended using a scaled-weighted averaging function.

#### Aggregation:

- Aggregation is done first per or satellite scene of interest for the desired time period. The products are simultaneously reprojected to a planetary lat/lon grid.
- Mosaicking. For larger areas, individual satellite scenes are mosaicked after temporal aggregation. For smaller areas, mosaicking can be combined with temporal aggregation.

### 3.3. Specific algorithms for Calimnos for coastal water quality

#### 3.3.1. General considerations

The following general considerations guided the algorithm selection for coastal waters:

- *Calimnos* is able to accommodate multiple atmospheric correction approaches. Recent analyses suggest that two approaches would be appropriate for OLCI retrievals in coastal waters (Mograne et al., 2019); the Case 2 regional coast colour neural network (C2RCC, Brockmann et al., 2016) alternative neural network (ANN) and the HyGEOS Polymer algorithm (Steinmetz et al., 2011). The ANN implementation of the C2RCC algorithm was not available at the start of TAPAS (only being introduced in 2019) while Polymer allows retrieval under sun-glint areas, a particular issue in the case of MERIS data, which was used extensively for matchup extraction in support of algorithm tuning. Consequently, Polymer was selected.
- We implement the options to include mineral absorption (available in the recent version of Polymer), as it improved the capacity of the bio-optical model to effect retrievals in turbid coastal environments (Jin et al., 2019), which was confirmed in the TAPAS case study site of Bourgneuf Bay.
- System vicarious calibration (SVC) gains were applied to remote sensing reflectance retrieved by OLCI-A. Similar gain corrections are not yet available for OLCI-B, so SVC gains are set to 1. Ongoing analysis of the radiometric performance of OLCI-B suggests that its behaviour is more similar to MERIS (the reference sensor) than OLCI-A. However, this is expected to introduce a bias on OLCI-B retrievals.

TAPAS exploits data from two ocean colour sensors; the Medium Resolution Imaging Spectrometer (MERIS), which flew aboard ENVISAT from 2002 to 2012, and its antecedent, the Ocean and Land Colour Instrument (OLCI), which is currently in operations aboard on the Copernicus Sentinel-3A (since 2016) and Sentinel-3B (since 2018). While there are other ocean colour sensors in operations (e.g. MODIS, VIIRS) and some optical sensors designed for land but with developing coastal applications (Landsat-8, Sentinel-2 MSI), OLCI offers the optimum combination of medium spatial resolution (300 m), high spectral resolution (21 bands), narrow spectral band width (typically 10 nm), optimized signal to noise, and frequent revisit times (~twice per day) required for coastal ocean applications.

Plymouth Marine Laboratory (PML) operationally downloads the entire OLCI Level-1B near-real time and non-time-critical full resolution (300 m) archive for Sentinel-3A and 3B. In addition, PML keeps a full archive of the full resolution (300 m) MERIS Level-1B catalogue with corrected latitude and longitude bands generated through the AMORGOS software. Downloaded data are described in a geospatial database to support spatial queries and calculation of relevant overpasses for a given target area.

#### 3.3.2. Pixel identification

The cloud detection function of the Idepix algorithm developed by Brockmann Consult was used in several processing chains, e.g. those used in CoastColour L1P and Diversity II.

Meanwhile many steps of the Idepix algorithm are included in the upcoming MERIS 4th reprocessing as standard algorithm by ESA. Due to the good performance of Idepix cloud screening in these applications, it is also selected for Calimnos. Idepix is based on a cloud probability derived from a neural net which has been trained with >60,000 manually classified pixels and which is combined with a number of additional tests on e.g. brightness, whiteness, glint. After clouds have been identified, a buffer can be defined in order to provide for a safety margin along cloud borders. This buffer radius (in pixel) can be parameterized and is set to 2 pixels.

Validation is performed by applying the PixBox Validation, a procedure where manually selected pixels are categorized to different categories and characterized with expert knowledge, e.g. to clear land, clear water, totally cloudy, semi-transparent cloud, cloud shadow, snow/ice, etc. A set of 17k MERIS FR pixels was collected in the scope of the CoastColour project, and detailed validation results are provided in the corresponding report (Ruescas et al., 2014).

Retrieval of water quality parameters is also strongly influenced by the occurrence of cloud shadow, which need to be identified and eliminated from further processing. Potential cloud shadow areas are identified by the geometry of the sun angle, viewing angle and the cloud height and the cloud bottom. The cloud height is gained by either the pressure or the temperature, but if this information is missing (not all sensors offer the respective bands), a maximum cloud height needs to be defined. The most difficult prediction is the height of the cloud base as it is not seen by the sensor. In Idepix it is defined as the minimum cloud height detected within the respective cloud minus an offset. The basis of cloud shadow detection is reliable cloud detection. Validation of the cloud shadow detection is done by visual inspection of different images under different conditions (cloud types and geometries).

In general, the most progressive combination of available cloud masks is selected, favouring accuracy over observation coverage.

Configuration: Idepix.Sentinel3.Olci v1.0

### 3.3.3. Atmospheric correction

POLYMER v4.12 is the latest version of an atmospheric correction processor initially designed to resolve water-leaving reflectance in clear ocean (case-1) waters including areas affected by sun glint (Steinmetz et al. 2011). The versatility of the processor to deal with bright waters has tested positively with a variety of optically complex (including inland) waters compared to alternative processors (Qin et al. 2017, Warren et al. 2019), although systematic underestimation of reflectance is evident in inland waters and overestimation of short wavebands is common. POLYMER applies a spectral optimization based on bio-optical model in conjunction with radiative transfer models to separate atmospheric (including glint) and water reflectance. The principle of the algorithm is a spectral matching method using a polynomial to model the spectral reflectance of the atmosphere and sun glint, and a bio-optical forward reflectance model for the water part. The algorithm uses the full set of wavebands available (user-configurable) as opposed to alternative ocean-colour methods that primarily extrapolate from near infra-red bands. The output is the fully normalized water-leaving reflectance per waveband.

Configuration:

- POLYMER according to Steinmetz et al. (2011), updated in Steinmetz (2016 and 2018), parameterized to use the Park and Ruddick (2005) bidirectional reflectance distribution function and operating only on pixels identified as water by the *Idepix* module (masks generated by POLYMER are not used). Starting conditions for the optimization procedure are set to chlorophyll-a = 1 mg m<sup>-3</sup> and total suspended matter = 1 g m<sup>-3</sup>. For the coastal seas configuration, a mineral absorption component included in the bio-optical model.

### 3.4. Specific algorithms for derived water quality products

#### 3.4.1. Optical water type (OWT) membership – overview

The OWT classification module in *Calimnos* was written at PML based on the work of Moore et al. (2001) and equivalent software developed for ESA Ocean Colour cci. *Calimnos* can be configured with an OWT set for lakes, defined in the GloboLakes project by the University of Stirling (Spyrakos et al. 2018), or it can use the new coastal OWT set described in the next section. In contrast to OWT mapping used in earlier versions of *Calimnos*, the spectral angle (Kruse et al. 1993) rather than Mahalanobis distance is selected as metric for similarity between spectra. The spectral angle is here defined over a range of 0 to 1 where 1 implies identical spectra.

#### 3.4.2. Generating a coastal optical water typology

Optical water typing allows for images to be classified according to some spectral parameter, such as spectral shape (Moore et al., 2009). However, this method is contingent on the existence of a library of pre-existing representative spectra, associated with the optical water types (OWT). While OWTs can be generated from in situ data (e.g. in Spyrakos et al., 2018) these types are not necessarily directly applicable to remote sensing sources. Alternative approaches using remote sensing spectra have been developed within the context of the OC-CCI programme (Jackson et al., 2017), but not to accommodate the full optical variability in coastal waters. The approach here is to extend this approach to coastal context, using a fuzzy classifier to iteratively identify the dominant clusters associated with the representative spectra.

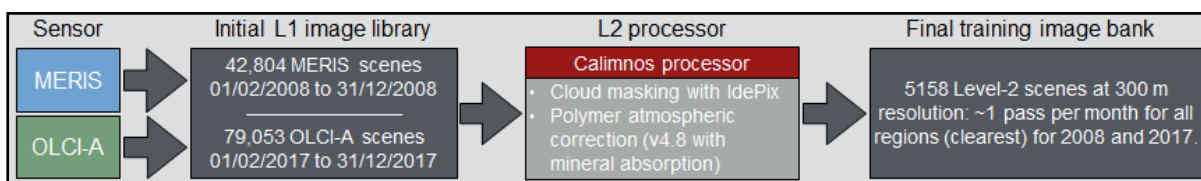


Figure 3: Construction and filtering of the initial image library.

The training dataset benefits from the inclusion of a global sampling of spectral variability. Consequently, OLCI-A and MERIS data were extracted over specific sites, representing this variability, as shown in Figure 4. These regions capture a diverse selection of turbid conditions (e.g. the North Sea, Amazon outflow and Yellow Sea), biologically active sites (e.g. Benguela upwelling, Great Lakes, Baltic Sea), open ocean (e.g. Hawaii and Bermuda) and polar conditions. One year of MERIS and one year of OLCI-A were extracted and processed for each of these sites, and filtered according to Figure 3.

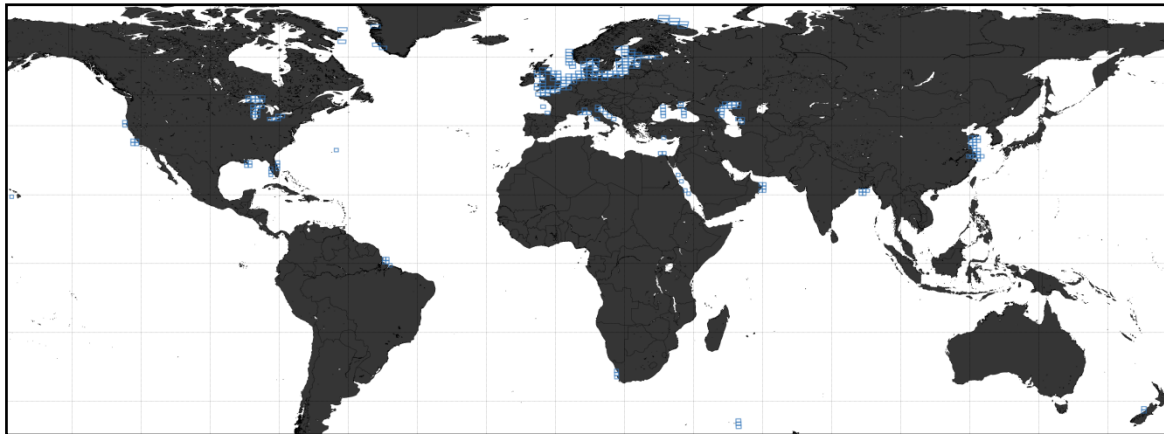


Figure 4: Regions used to construct the spectral library for optical water type determination. Areas were selected due to presence of unique spectral signatures associated with high suspended sediment concentrations, the occurrence of specific algal species, or both. Selected areas include: the Amazon outflow, the Labrador Sea, Hawaii (HOTS), Bermuda (BATS), the Great Lakes, the Benguela, Kerguelin, the Red Sea, the Gulf of Oman, the Yellow Sea, the Bay of Bengal, the Black Sea, the Caspian Sea, the Mediterranean Sea, the North Sea, the Baltic Sea, the White Sea, the Florida Coast, the California Coast and the New Zealand Coast.

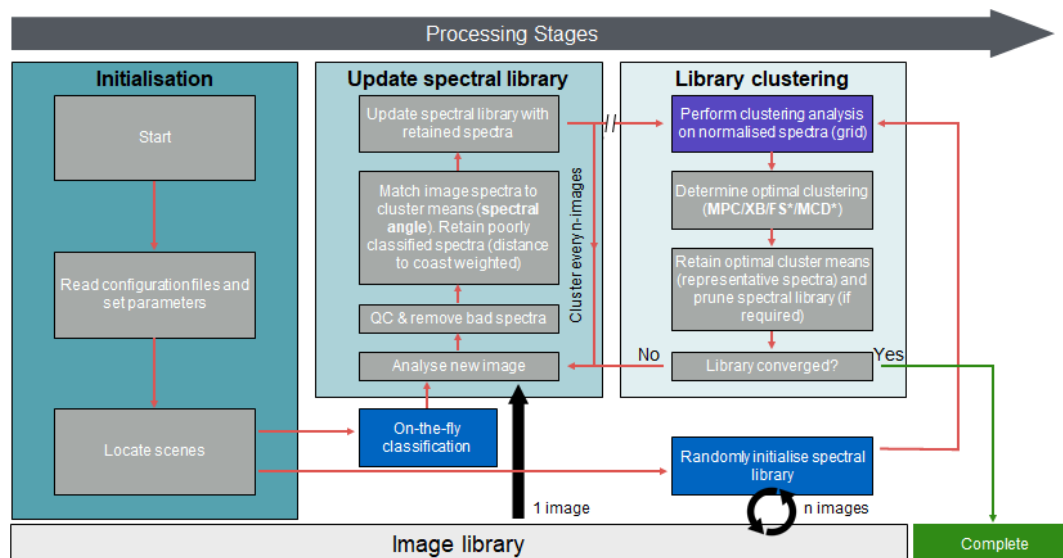


Figure 5: Schematic of the optimisation system used to iteratively classify the spectral library into representative spectra corresponding to the optical water types.

The filtered image library contains over two billion atmospherically corrected water-leaving radiance reflectance spectra. Performing a cluster analysis on such a large multi-channel dataset is not feasible, so an iterative approach is introduced to identify clusters (Figure 5). This approach begins with a selection of spectra from a randomly selected subset of images. To emphasize coastal variability, pixels nearer the coast are given a stronger selection weighting while rejecting pixels immediately adjacent to land (where possible, as cloud may impact the ability to test this criterion). The following bands are used in the cluster analysis: 412.5 nm, 442 nm, 490 nm, 510 nm, 560 nm, 620 nm, 665 nm, 681 nm, 709 nm, 765 nm, 778 nm, 865 nm, 885 nm, 900 nm.

After the initial library is instantiated it is subjected to a fuzzy cluster analysis, using a combination of the Xie-Beni index and Modified Partition Coefficient to identify the optimal clustering. The top 100,000 library spectra that best correspond to each representative

cluster type are then stored while all other spectra are discarded. Subsequently, the next  $n$ -images (with  $n=10$ , typically) are assessed against the cluster types using spectral angle as the comparative metric. Spectra that poorly match the existing database are retained, provided they satisfy quality control requirements that preclude extreme, likely non-physical, reflectances. The resulting spectral library is then reclassified and the same retention/discard criteria are applied. This process is repeated until the number of clusters and cluster scores converge (Figure 6). This process takes typically four hours to assess  $\sim 1000$  images. Given the random nature of the initial library selection, and the propensity of clustering approaches to be highly subject to initial conditions, the process was repeated several times to ensure that the final set of clusters was robust.

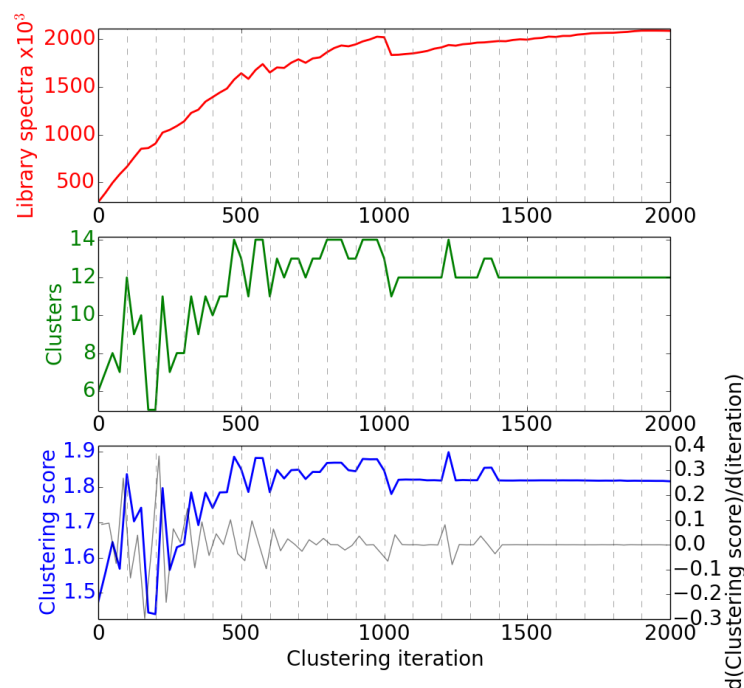


Figure 6: Convergence of the optical water type cluster algorithm.

The spectral library consistently converged on 12 clusters with representative spectra shown in Figure 7. Each of these representative spectra is assigned a numeric optical water type. These optical water types form the basis of the partitioning used to under-pin algorithm selection and blending in the TAPAS products.

To test the veracity of the clustering approach two further tests were conducted. In the first test, the iterative clustering approach was applied to a synthetic spectral library constructed only of randomly distributed instances of each of the 12 representative spectra. The clustering approach correctly retrieved all 12 classes. Next, systematic noise was added to the synthetic spectral library to determine how resilient the approach may be to small scale signals. The clustering proved resilient up to the point that the signal to noise ratio reached approximately 2:1.

As the optical water types are derived from remotely sensed spectra rather than in situ observations, it is not possible to directly attribute the classes to water-column properties. Attribution requires an independent data set of in situ measurements of optically active water constituent concentrations and/or inherent optical properties. For the time being, based on



spectral shape the spectra and their spatial distribution, Table 1 gives a suggested qualitative interpretation of how the most common types relate to optical-biogeochemical conditions.

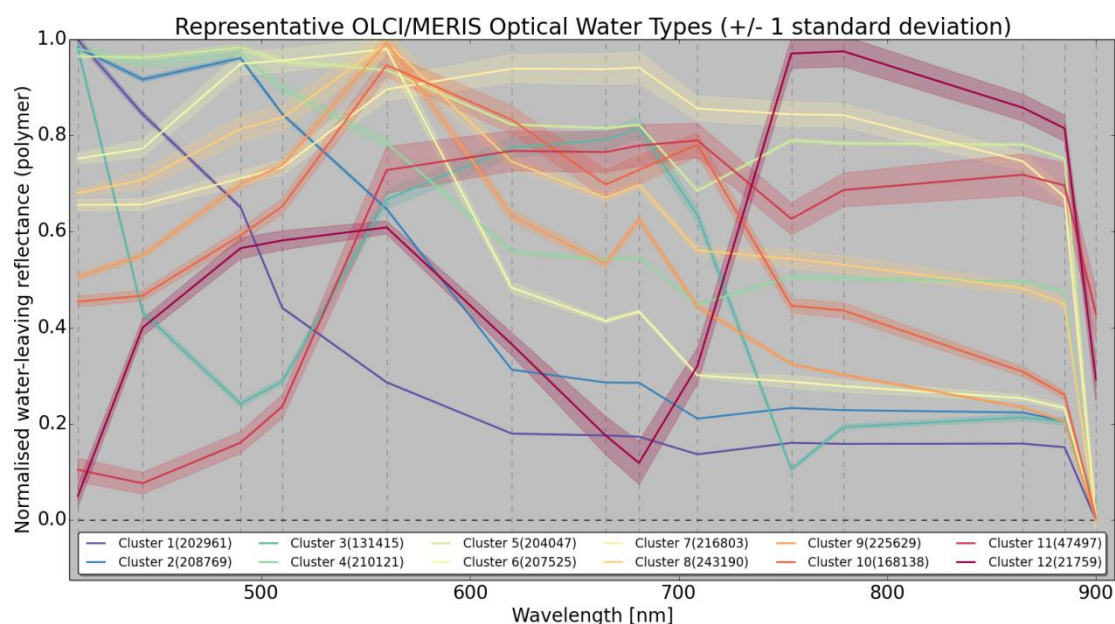


Figure 7: The representative spectra corresponding to the optical water types. The spectra are shown as normalised.

Table 1: Qualitative interpretation of the representative spectra associated with the optical water types prevalent in UK waters. Shading matches the relevant spectral colour in Figure 7

Optical water type	Qualitative interpretation
1	Clear blue waters
2	Blue/transitional waters; slightly increased scattering
6	Coastal scattering
9	Strong coastal scattering
10	Very strong coastal scattering
11	Extremely strong coastal/estuarine scattering
12	High NIR, likely affected by adjacent land

Examples of the spatial distribution of the dominant optical water types are shown in Figure 8. It should be noted that these maps shows the dominant optical water type in each pixel, i.e. the most similar optical water type based on the spectral angle metric.

From Figure 8 it appears clear that the optical water typology appropriately renders the transition between clear blue open waters (OWT 1), through moderately scattering coastal environments (OWT 6/9) to highly scattering environments in estuarine areas (OWT 10/11).

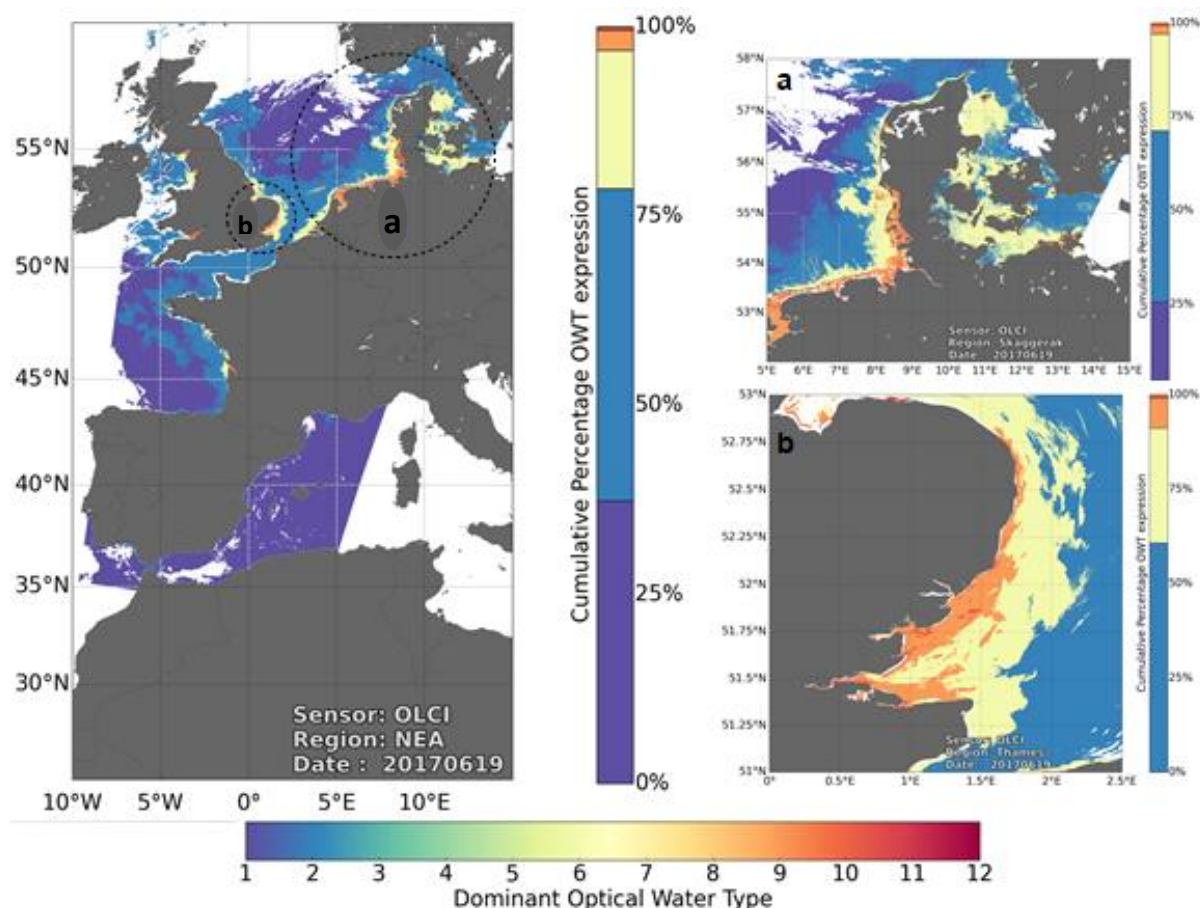


Figure 8: Mapping of the dominant optical water type for the North East Atlantic region on 19/06/2017.

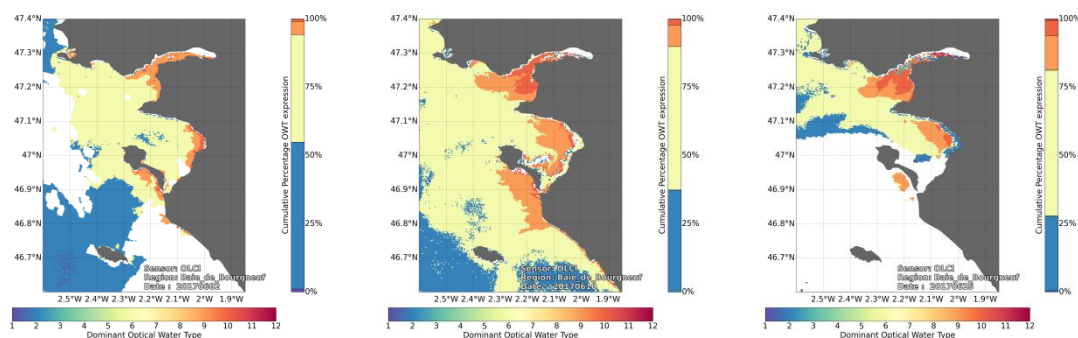


Figure 9: Example evolution of the dominant optical water type across the Bourgneuf Bay in June 2017.

### 3.4.3. Algorithm selection, tuning, calibration and validation:

Algorithms for all retrieved parameters are selected and tuned according to a partitioning of the spectral variability of the region by optical water typing. An initial example of tuning of both Chl-a and TSM algorithms was shown in Section 2. Here, we present a more advanced version of tuned TSM and turbidity algorithms, applied to each optical water type (OWT) are shown in Table 2. A similar exercise for Chl-a re-tuning will be required. Over 95% of the pixels assessed correspond to optical water types 1, 2, 6, 9 and 10 (Figure 10).



**Table 2: Algorithms associated with each optical water type. N/A indicates that no points corresponding to this OWT are available in the calibration data set.**

Optical Water type	Turbidity Algorithm	TSM algorithm
1	Nechad et al. (2009) @ 681 nm	Tang et al. (2013) @ 681
2	Nechad et al. (2009) @ 681 nm	Tang et al. (2013) @ 560
3	N/A	N/A
4	N/A	N/A
5	N/A	N/A
6	Nechad et al. (2009) @ 620 nm	Nechad et al. (2009) @ 620 nm
7	N/A	N/A
8	N/A	N/A
9	Nechad et al. (2009) @ 779 nm	Zhang et al. (2014) @ 509
10	Nechad et al. (2009) @ 779 nm	Nechad et al. (2009) @ 779 nm
11	N/A	N/A
12	N/A	N/A

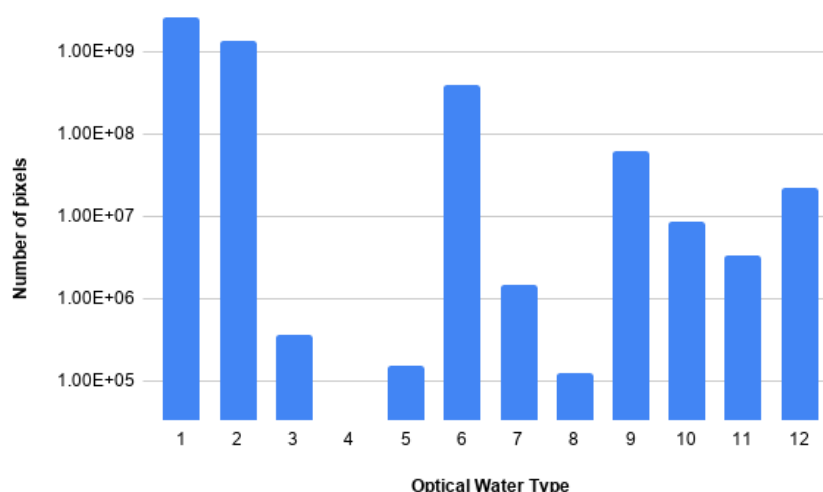


**Figure 10: Number of pixels corresponding to each optical water type between June to August 2019 (shown on a log scale). In total 18.4% of pixels are categorised, with the remainder discarded due to invalidity, land, or, most frequently, cloud.**

**Table 3: Sources of data used for calibration/validation of TAPAS TSM and turbidity algorithms.**

Source	Variables	Num obs.	Date start	Date end
CEFAS smart buoy data	Coastal and open ocean TSM and turbidity	TSM: 537,349 TURB: 1,258,804	01-01-2002	15-08-2018
OC-CCI in situ record	Coastal and open ocean TSM	TSM: 6,451	02-01-1997	03-07-2012
SEPA	Estuarine turbidity	TURB:1,207,950	01-01-2005	31-12-2017

Algorithm calibration and validation was performed using data from the sources detailed in Table 3. These stations cover both coastal and offshore locations, ensuring relevance to the full suite of optical water types encountered in the region. The data set was split into two parts, with 25% of the initial points used to calibrate the relevant algorithms and the remaining data used for validation across the calibration period, to ensure that the calibration and validation data sets are independent calibration and validation points are selected so that they do not fall on the same day for the same datasets (giving at least one tidal cycle between

any calibration and validation point for each data set). Match-up extractions were performed using only the nearest image pixel, and with in situ data only +/- 30 minutes from the relevant overpass time. Pixel flags were applied, as recommended in Bailey and Werdell (2005), but, as significant spatial variability is to be expected in the coastal zone, no spatial averaging, or filtering by a coefficient of variation are performed (sic). The locations of the in situ match up points used for calibration/validation are shown in Figure 11.

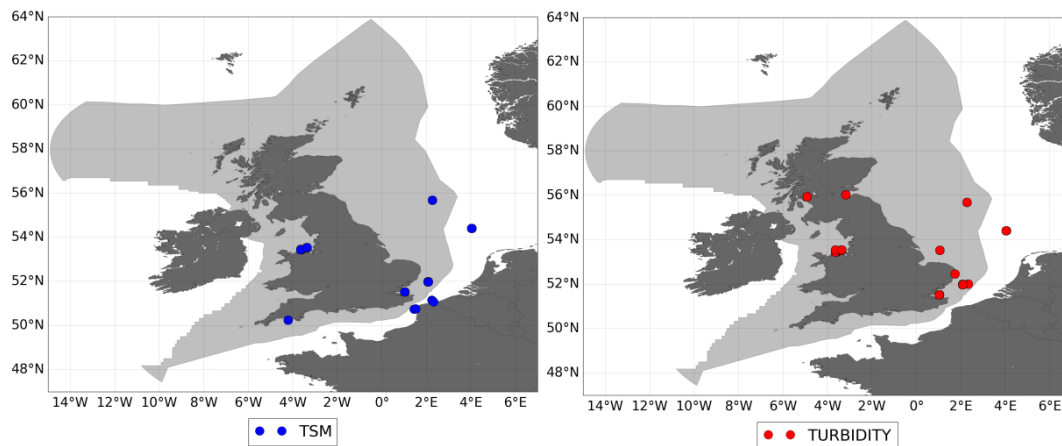


Figure 11: Locations of match-up points used in calibration and validation.

The results of the algorithm calibration and validation for the TSM and turbidity retrieval algorithms are shown in Figure 12 and Figure 13, respectively. The middle panel in each figure shows the results of validation when only the dominant algorithm for each water type is used. The right hand panel shows the results for the case when the top 2 algorithms are blended together according to the fuzzy membership of the relevant spectra to each optical water type. This latter approach reduces the hard spatial boundaries between algorithms often associated with the classical switching approaches.

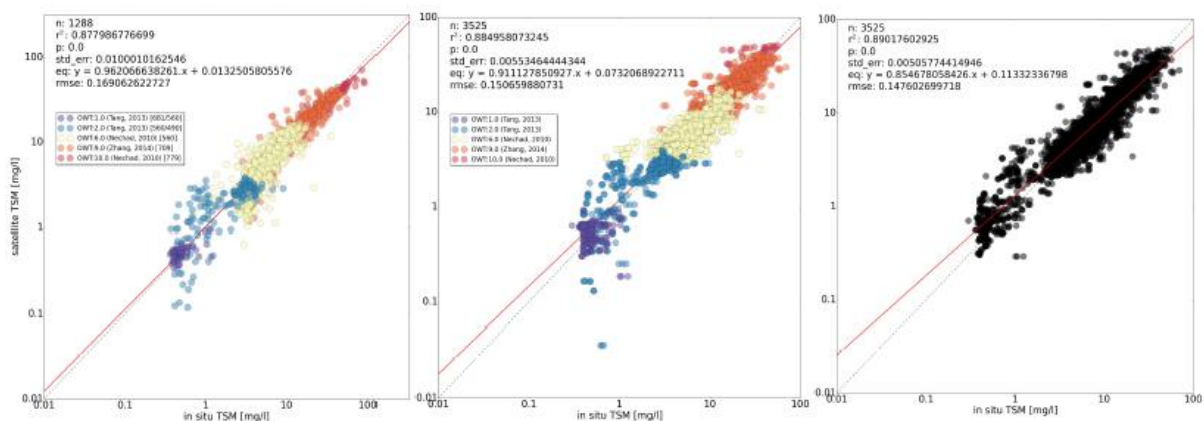


Figure 12: (left) TSM calibration by optical water type algorithm. (centre) TSM validation by optical water type. (right) TSM validation for the blended algorithm.

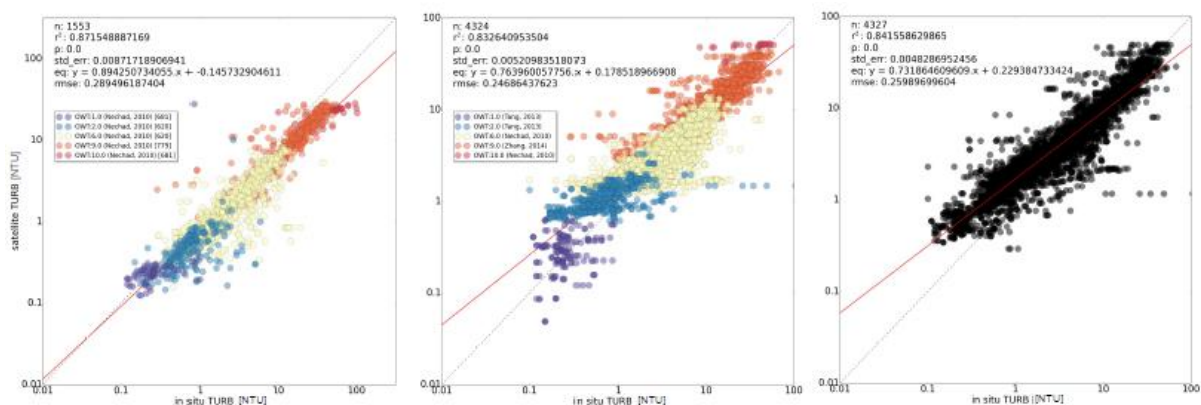


Figure 13: As in Figure 12, but for turbidity. Note that, for consistency, where the optical water type suggests that one of the Neckad algorithms is used to derive TSM, the same algorithm is used to derive turbidity. This is because the Neckad algorithm derives a value for TSM by applying a geometric factor to the retrieved turbidity.

### 3.4.4. Limitations, recommendations for use and further evolution of the algorithm

We note the following known limitations of the current approach:

- Not all optical water types are represented in European waters, and not all optical water types of those identified in European waters have corresponding in situ match-up data.
- If no matching satellite and in situ observations are available to select/tune an algorithm, then no TSM/turbidity can be retrieved for that optical water type. Since each pixel has a similarity score corresponding to each possible optical water type, a value will normally be reported for that pixel regardless of missing inputs, but likely with a higher associated uncertainty.
- Uncertainties are calculated for each pixel. These are extracted from the residual of each algorithm regression against in situ data, and consequently, vary with retrieved concentration. Consequently, an incorrect assignment of an optical water type to a given pixel, and therefore a poor retrieval is likely to result in a high uncertainty.

Product uncertainty is closely tied to the calibration and validation procedures:

- Increased availability of in situ data over time is expected to expand the ability to retrieve water quality products for as-yet unassigned optical water types.
- Beyond the initial validation exercise, which incorporated the MERIS and first two years of the OLCI-A mission, a subsequent validation has been conducted. This secondary validation exercise assesses the performance of the turbidity algorithm over the July 2018 to June 2019 period for both OLCI-A and OLCI-B. During this period, the performance of the blended products is not as strong as during the initial calibration/validation phase due to the lack of SVC gains for S3B and poorer quality control on the near-real time in situ data, as compared to the historical CEFAS SmartBuoy data used in the original exercise. However, the blended algorithm continues to outperform all other approaches.

Users are strongly recommended to use the blended algorithm result, which removes unrealistic boundaries otherwise introduced by applying individual algorithms beyond their validated scope:

- The blended algorithms for both turbidity and TSM show improved performance over any single algorithm and as well as over using only the algorithm associated with just the dominant optical water type.
- The blending process greatly reduces the spatial inhomogeneity associated with the use of any single algorithm.
- Like the retrieved parameters themselves, the uncertainties are geometrically blended according to the scores of each pixel against each of the top-three performing algorithms.

### 3.5. Output product

The output data (product bands) are produced as variables in a NetCDF file. Variables include a band for each reflectance band, the derived chlorophyll-a and turbidity and the associated pixel uncertainty for each of these. Intermediary products are not distributed but are generally stored for product validation and improvement purposes. These include the specific outputs from individual algorithms (prior to mapping/blending) and processor-generated flags.

Figure 14 shows an example OWT-blended TSM product for the North East Atlantic region for 24/08/2019. The daily aggregated product retains a spatial resolution of 300 m can be used as the basis for time series extractions and statistical analysis of any subset region. A similar analysis is conducted for the Mediterranean Sea.

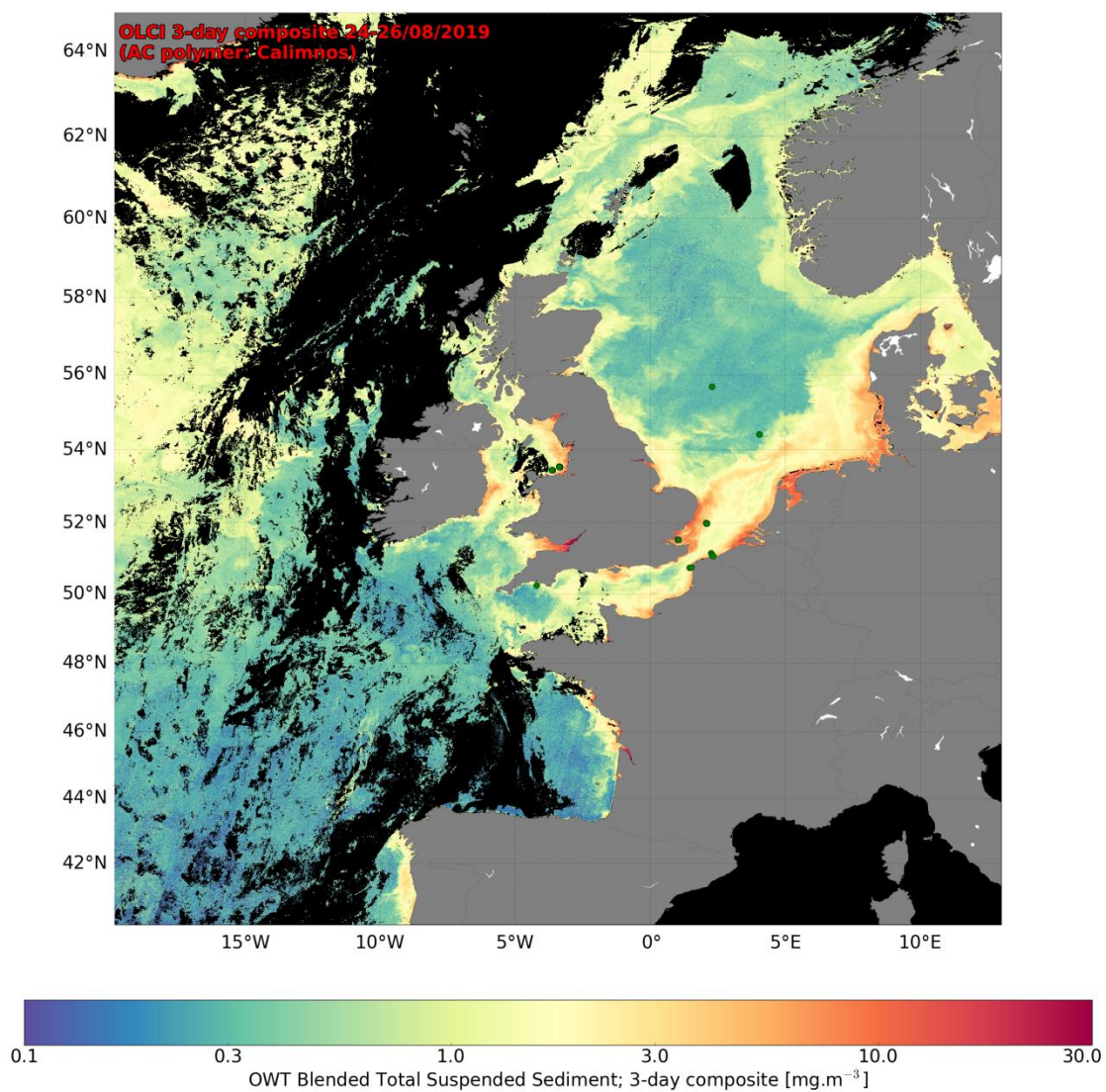


**Figure 14: An example OWT blended, 3-day aggregated Total Suspended Matter product for 24-26 Aug 2019.**



## 4. The S3 processing chain for Bourgneuf Bay (Water Insight)

### 4.1. Background

For Partner UN Water Insight has started a first Sentinel 3 OLCI processing chain for the area of Bourgneuf Bay to compare to their MERIS processing results. The area of Bourgneuf Bay is limited by the following bounding box:

UL, 47.326 N, -2.535 E

UR, 47.350 N, -1.748 E

LR, 46.873 N, -1.7839 E

LL, 46.867 N, -2.476 E

The area and its aquaculture sites are already described in section 2.1.

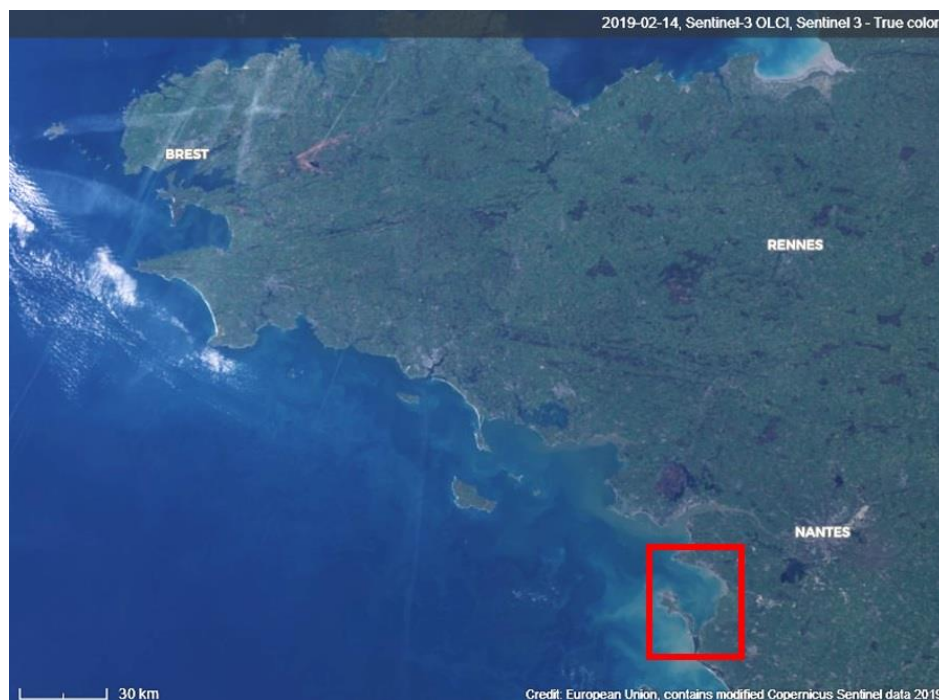


Figure 15: The Bourgneuf Bay study area

WI has set up this processing chain as one of its first S3 processing services at the time, as S3 was relatively new.

### 4.2. S3 processing chain

The WI processing chain consists of four steps: the automatic downloading, the atmospheric correction, the application of the water quality algorithms for chlorophyll-a, suspended particulate matter, and transparency (Kd) and the service delivery.

Sentinel 3 OLCI imagery was downloaded for the period between 27/01/2017 and 13/10/2017 using the EUMETSAT's earth observation portal and a Water Insight automated downloading script.

For atmospheric correction, the same correction was used as described above in chapter 3; the POLYMER v4.5 (Steinmetz et al 2011) method. The output bands contain the water reflectance (dimensionless, fully normalized for sun and sensor at nadir. The flagging of the invalid pixels (due to land, clouds etc) was done using the built-in flag mask called bitmask which is automatically calculated during the atmospheric correction.

Chlorophyll and SPM water quality parameters were calculated using the algorithms below.

- Novoa SPM According to Novoa et al 2017
- GONS CHL According to Gons et al 2015
- OC4ME CHL According to <https://sentinels.copernicus.eu/web/sentinel/technical-guides/sentinel-3-olci/level-2/oc4me-chlorophyll> (Morel et al 2007 and O'Reilly et al 1998 for a more general description of the algorithm)
- Turbidity Nechad 665
- Turbidity Nechad 754
- Turbidity Nechad 865
- Turbidity Nechad 1020

These algorithms were selected as state-of-art algorithms suitable for the optical water types in the area.

As discussed in section 2, UN used the MERIS results to quantitatively assess which type of regional algorithms perform best for aquaculture sites in Bourgneuf Bay. It is expected that updated regional algorithms could be applied to S3 (as the OLCI sensor is based on the MERIS sensor). The validation of S3 is still on-going as it requires in-situ measurements. The deployment of a turbidity and chlorophyll-a probe by UN has been delayed. A first trial of deployment at an offshore site was a failure due to a wrong move by the boat captain during the deployment of the instrument cage. The probe has been buried in the sediment, but we figured it out only months later when we retrieved the instrument. As a consequence, there is no in situ data concomitant with the S3 images processed by WI. Our in situ probe has been rescued, checked, re-calibrated, and eventually re-deployed in an intertidal oyster farming site, very recently. All analyses will therefore be performed after the official end of TAPAS.

## 5. Conclusions and recommendations

The potential to use the Sentinel-3 OLCI instrument for monitoring water quality in aquaculture environments has been investigated. Atmospheric corrections processors have been compared and several retrieval algorithms were optimised (largely based on the performance of MERIS, the predecessor of OLCI). Based on validation results, the most suitable combinations of algorithms were selected for processing data sets of two test sites.

The results are mostly positive: OLCI is capable of resolving the optical dynamics present in aquaculture environments. Atmospheric correction can be further improved, and algorithm validation is limited by available in situ data. The number of radiometric in situ observations for validation could be improved.

The medium resolution satellite data can be used for improved spatial planning (e.g. site selection and characterisation), impact assessment and licencing, and enhanced monitoring e.g. for early warnings. Some tests for these purposes have already been performed. After the current work the high-resolution data is ready for testing the application in aquaculture tools at other aquaculture sites.



## 6. References

- Adams, T. P., R. G. Miller, D. Aleynik, and M. T. Burrows, Offshore marine renewable energy devices as stepping stones across biogeographical boundaries. *Journal of Applied Ecology*, 51(2), 330-338, doi:10.1111/1365-2664.12207, 2014.
- Bicheron, P., Amberg, V., Bourg, L., Petit, D., Huc, M., Miras, B., Arino, O. (2011): Geolocation Assessment of MERIS GlobCover Orthorectified Products. *IEEE Trans Geosci Remote Sens*, 49(8), 2972–2982.
- Binding, C.E., J. H. Jerome, R. P. Bukata & W. G. Booty. (2010): Suspended particulate matter in Lake Erie derived from MODIS aquatic colour imagery. *International Journal of Remote Sensing* 31(19).
- Bouvet M., Ramoino F. (2010): Equalization of MERIS L1b products from the 2nd reprocessing, ESA TN TEC-EEP/2009.521/MB.
- Diversity-II (2015): ESA DUE DIVERSITY II- Algorithm Theoretic Baseline Document (ATBD), Version 2.4, [http://www.diversity2.info/products/documents/DEL5/DIV2\\_Algorithm\\_Theoretical\\_Basis\\_Document\\_v2.4.pdf](http://www.diversity2.info/products/documents/DEL5/DIV2_Algorithm_Theoretical_Basis_Document_v2.4.pdf).
- Falconer, L., Middelboe, A.L., Kaas, H., Ross, L.G., Telfer, T.C. (2019). Use of geographic information systems for aquaculture and recommendations for development of spatial tools. *Rev. Aquacult.* doi: 10.1111/raq.12345
- Gernez, P., Doxaran, D., Barillé, L. (2017). Shellfish aquaculture from space: potential of Sentinel2 to monitor tide-driven changes in turbidity, chlorophyll concentration and oyster physiological response at the scale of an oyster farm. *Front. Mar. Sci.* 4, 137. doi: 10.3389/fmars.2017.00137
- Gohin F., J. N. Druon & L. Lampert (2002) A five channel chlorophyll concentration algorithm applied to SeaWiFS data processed by SeaDAS in coastal waters, *International Journal of Remote Sensing*, 23:8, 1639-1661, DOI: 10.1080/01431160110071879
- Gons, H. -J., Rijkeboer, M., & Ruddick, K. -G. (2005). Effect of a waveband shift on chlorophyll retrieval from MERIS imagery of inland and coastal waters. *Journal of Plankton Research*, 27, 125–127.
- Gordon, H. R., O. B. Brown, R. H. Evans, J. W. Brown, R. C. Smith, K. S. Baker, and D. K. Clark. (1988): A semianalytic radiance model of ocean color. *J Geophys Res: Atmos* 93: 10909-10924.
- Kruse F.A., A.B. Lefkoff, J.W. Boardman, K.B. Heidebrecht, A.T. Shapiro, P.J. Barloon, A.F.H. Goetz. (1993): The spectral image processing system (SIPS)—interactive visualization and analysis of imaging spectrometer data, *Remote Sens Environ*, 44(2–3):145-163.
- Moore, TS., JW. Campbell and Hui Feng. (2001): A fuzzy logic classification scheme for selecting and blending satellite ocean color algorithms. *IEEE Transactions on Geoscience and Remote Sens* 39(8) 1764-1776.
- Morel, A. (1974). Optical properties of pure water and pure sea water. In: Jerlov MG, Nielsen ES, editors. *Optical Aspects of Oceanography*. New York: Academic Press; 1974. p. 1–24.
- Morel, A., Gentili, B., Claustre, H., Babin, M., Bricaud, A., Ras, J., et al. (2007). Optical properties of the "clearest" natural waters. *Limnology and Oceanography*, 52, 217-229.
- Nechad, B., Dogliotti, A.I., Ruddick, K.G., Doxaran, D., (2016): Particulate Backscattering and suspended matter concentration retrieval from remote-sensed turbidity in various coastal and riverine turbid waters. *Proceedings of ESA Living Planet Symposium, Prague, 9-13 May 2016, ESA-SP 740*.
- Nechad, B., Ruddick, K.G, Park, Y. (2010): Calibration and validation of a generic multisensor algorithm for mapping of total suspended matter in turbid waters". *Remote Sens Environ* 114 (2010) 854–866.

- Novoa, Stéfani & Doxaran, David & Ody, A. & Vanhellemont, Quinten & Lafon, Virginie & Lubac, Bertrand & Gernez, Pierre. (2017). Atmospheric Corrections and Multi-Conditional Algorithm for Multi-Sensor Remote Sensing of Suspended Particulate Matter in Low-to-High Turbidity Levels Coastal Waters. *Remote Sensing*. 9. 10.3390/rs9010061.
- O'Reilly, J.E., Maritorena, S., Siegel, D.A., O'Brien, M.C., Toole, D., Mitchell, B.G., et al. (2000). Ocean color chlorophyll a algorithms for SeaWiFS, OC2, and OC4: Version 4. SeaWiFS postlaunch calibration and validation analyses, Part, 3, pp.9-23.
- Palmer S, Gernez P, Thomas Y, Simis S, Miller P, Glize P, and Barillé L. (accepted). Remote sensing-driven Pacific oyster (*Crassostrea gigas*) growth modelling to inform offshore aquaculture site selection. *Frontiers in Marine Sciences*. doi: 10.3389/fmars.2019.00802
- Park Y.J. and Ruddick K. Model of remote-sensing reflectance including bidirectional effects for case 1 and case 2 waters. (2005): *Appl Optics*. 2005;44(7):1236-49. doi: 10.1364/ao.44.001236
- Roettgers, R., Doerffer, R., McKee, D. and Schoenfeld, W. (2011): Pure water spectral absorption, scattering, and real part of refractive index model. ESA Water radiance project. From [www.brockmann-consult.de/beam-wiki/download/attachments/17563679/WOPP.zip?version=1&modificationDate=1299075673760](http://www.brockmann-consult.de/beam-wiki/download/attachments/17563679/WOPP.zip?version=1&modificationDate=1299075673760)
- Ruescas, A. B., Brockmann, C., Stelzer, K., Tilstone, G. H., Beltran, J. (2014): DUE CoastColour Validation Report (p. 58). Geesthacht, Germany: Brockmann Consult. Retrieved from [http://www.coastcolour.org/documents/DEL-27%20Validation%20Report\\_v1.pdf](http://www.coastcolour.org/documents/DEL-27%20Validation%20Report_v1.pdf).
- Simis, S., Stelzer, K., Müller, D. (2018). Copernicus Global Land Operations "Cryosphere and Water" "CGLOPS-2" Framework Service Contract N° 199496 (JRC): Lake waters 300m and 1km products. Version 1.2.0, Issue I1.08.
- Spyrakos E, O'Donnell R, Hunter PD, Miller C, Scott M, Simis S, et al. (2018): Optical types of inland and coastal waters. *Limnol Oceanogr*. 63(2). doi: 10.1002/lno.10674.
- Steinmetz F, Deschamps P-Y, Ramon D. Atmospheric correction in presence of sun glint: application to MERIS. (2011): *Optics Express*. 19(10):9783-800. doi: 10.1364/oe.19.009783
- Steinmetz, F. Ramon, D., Deschamps, P-Y (2016): ATBD v1 – Polymer atmospheric correction algorithm, D2.3 OC-CCI project [http://www.esa-oceancolour-cci.org/?q=webfm\\_send/658](http://www.esa-oceancolour-cci.org/?q=webfm_send/658)
- Steinmetz, F. (2018): ATBD v1 – Evolution of Polymer Atmospheric correction within Copernicus Global Land Service – Inland Water products. On request
- Qin P, Simis SGH, Tilstone GH. (2017): Radiometric validation of atmospheric correction for MERIS in the Baltic Sea based on continuous observations from ships and AERONET-OC. *Remote Sens Environ* 200:263-80.
- Warren MA, Simis SGH, Martinez-Vicente V, Poser K, Bresciani M, Alikas K, et al. (2019): Assessment of atmospheric correction algorithms for the Sentinel-2A MultiSpectral Imager over coastal and inland waters. *Remote Sens Environ* 225:267-89.

[End page leave blank]

UNIVERSITY of  
STIRLING



NIVA  
Norsk institutt for vannforskning

PML Plymouth Marine  
Laboratory



Marine Institute  
Foras na Mara



Aquaculture  
Stewardship  
Council



ALTERRA  
WAGENINGEN UR

idea  
water



UNIVERSITÉ DE NANTES

NACEE



SZENT ISTVÁN  
UNIVERSITY

